IEEE Access
Multidisciplinary ⋮ Rapid Review ⋮ Open Access Journal

Received January 4, 2020, accepted January 11, 2020, date of publication January 20, 2020, date of current version January 29, 2020.

Digital Object Identifier 10.1109/ACCESS.2020.2967886

Improved Distributed Predictive Functional Control With Basic Function and PID Control Structure

ZHE YU, JIANJUN BAI, AND HONGBO ZOU
Automation College, Hangzhou Dianzi University, Hangzhou 310018, China

Corresponding author: Hongbo Zou (zouhb@hdu.edu.cn)

This work was supported by the National Natural Science Foundation of China under Grant 61773146.

ABSTRACT It is known that constraints and disturbances in practice may affect the performance of distributed predictive functional control (DPFC) system greatly, thus it is necessary to develop a method to enhance the control performance further. Based on such background, a modified predictive functional control with basic function and PID control structure (BFPID-DPFC) is proposed for large-scale strong coupling system in this paper. In this approach, the performance index is reconstructed by utilizing the Proportional integral derivative (PID) factor and the weighting coefficient of basis functions firstly, then the ensemble control performance of the strong coupling system can be improved by adjusting the corresponding factors. Further, the coupling effect between subsystems can be eliminated by employing Nash game theory, then the improved DPFC approach is obtained. The comparisons between conventional DPFC method and the BFPID-DPFC approach are done in the simulation part, and the results show that the ensemble control performance of the proposed DPFC algorithm is better.

INDEX TERMS Distributed predictive functional control, PID control, basis function, coupling system.

I. INTRODUCTION

With the increasing control scale in practical industrial processes, the number of corresponding variables that need to be regulated has exceeded the handling ability of traditional model predictive control (MPC). Meanwhile, the control requirements in industry are also stricter, therefore, the relevant performance obtained by applying the conventional MPC may not be satisfactory [1], [2]. During the past decades, modern information technology has been developed greatly, and there are lots of progresses in the development of MPC. Among these improvements, distributed MPC (DMPC) that is formed by combining MPC and distributed control has been put forward for these large-scale multivariable strong coupling systems [3]–[6]. Research on the improvement of DMPC can provide some novel solutions for complex industrial control.

The studies on the DMPC are always hot topics, and there are many representative fruits. In order to solve the problem of trailer trajectory tracking, Kayacan *et al.* [7] designed a distributed nonlinear MPC algorithm. A novel distributed predictive controller, which can make the large-scale nonlinear system stable, was presented in [8]. Li *et al.* [9] studied the consistency of distributed receding horizon control and discussed how to use neighbor information to deal with the first-order multi-agent system. By selecting the formation of small unicycle as research object, a multi-level DMPC method was addressed [10]. Gao *et al.* [11] developed a cooperative DMPC scheme by studying the linear subsystems with coupling cost and coupling constraints. In [12], a detailed investigation on DMPC was done. A systematic research on network and DMPC was completed by Christofides *et al.* [13]. The DMPC has also been applied in practical processes, such as: Venkat *et al.* [14] investigated the application of DMPC in cooperative game, and the DMPC was applied to four-tank system by Mercangöz and Doyle [15].

As for PID control, it is one of the earliest and the most classic algorithms in industrial control. Because of its excellent characteristics, PID control has been widely used in practice [16], [17]. In PID control, the adjustment of three control parameters is particularly important, because these parameters influence the control accuracy greatly [18]. Ziegler and Nichols(Z-N) put forward the earliest PID tuning method, which is called Z-N tuning approach and has been accepted and used far and wide [19]. Based on Z-N tuning method,

The associate editor coordinating the review of this manuscript and approving it for publication was Dazhong Ma.

Cohen and Coon presented the C-C setting method [20]. After that, researcheon PID control and its tuning method are springing up. For the system with time-delay, Smith designed the predictive compensation controller [21]. On the basis of Smith controller, Fruehauf *et al.* [22] developed the internal model control algorithm. Astrom made a comprehensive study of self-tuning control and adaptive control, which contributes to the development of intelligent PID tuning significantly [23]. In [24], the authors presented Fuzzy Particle Swarm Optimization of PID controller as a Conventional Power System Stabilizer CPSS to improve the dynamic stability performance of generating unit during low frequency oscillations. Classic proportional-integral-derivative (PID) controller, fuzzy logic controller and PID-type Fuzzy adaptive controller methods were also proposed [25]. Besides, there are also many other crucial research on the combination of PID control and MPC approaches [26]–[29].

DPFC is one of the main branches of DMPC algorithms. In the design of DPFC, the large-scale system is divided according to the actual industrial process firstly. Then optimization is implemented for each subsystem. Meanwhile, the communication between subsystems is realized by the Nash game theory and the communication capability of computer, then the coupling effect among subsystems can be eliminated [30].The control circuits for DPFC were designed using line currents, series reference voltages and these are controlled by conventional controllers [31]. In [32], the authors presented four control methodologies to mitigate these difficulties using small-scale distributed battery storage. These four approaches represent three different control architectures: 1) centralized; 2) decentralized; and 3) distributed control. While in [30], the authors designs a distributed PID type dynamic matrix control method based on fractional order systems. A distributed model predictive control algorithm for heterogeneous vehicle platoons with unidirectional topologies and a priori unknown desired set point was presented in [33]. To solve the problem of complex online calculation in large scale predictive control system, the optimization algorithm based on Nash optimality for distributed predictive functional control was proposed [34]. In [35], the authors investigated the consensus problem of general linear discrete-time multi-agent systems using distributed model predictive control with self-triggered mechanism. However, the control performance of DPFC is deteriorated by the inevitable disturbance and constraints in the processes, and the corresponding performance may not meet the actual production requirements [36]–[40]. Thus, it is significant to develop an improved DPFC scheme to enhance the system performance.

To the author's knowledge, constraints and disturbances in practice may affect the performance of the distributed predictive functional control algorithm greatly. What's more, most existing research results only focus on the performance improvement of one aspect of the large-scale system. As to some processes with stricter requirements, the existing research results may be insufficient and need to be modified. To cope with such conditions, an enhanced DPFC strategy with basic function and PID control structure is developed in this article. By employing the PID factor and the weighting coefficient of the basis function, the new performance index is obtained. Then the ensemble performance of the large-scale strong coupling system can be improved by adjusting the corresponding factors. By introducing the Nash game theory, the DPFC is acquired through eliminating the coupling effect among the subsystems. The simulations verify the validity of the improved DPFC method finally.

This paper is organized as follows. In section 2, the derivation of the traditional DPFC algorithm is described, and the BFPID-DPFC algorithm is designed in section 3. In section 4, the relevant case studies on large-scale coupled system are introduced, and section 5 gives the conclusion.

II. TRADITIONAL DPFC

In this section, the DPFC is introduced through the corresponding derivations and the proof of its convergence theorem.

A. DERIVATIONS OF DPFC ALGORITHM

The main characteristic of large-scale system is that the input of one subsystem will affect the output of the other subsystems, and these coupling features make the relevant control complicated. Here, we suppose that the large-scale coupled system can be described as the following transfer function model with inputs and outputs [5], [14], [32].

$$G(s)=\begin{bmatrix}\frac{K_{11}e^{-\tau_{11}s}}{T_{11}s+1} & \frac{K_{12}e^{-\tau_{12}s}}{T_{12}s+1} & \cdots & \frac{K_{1N}e^{-\tau_{1N}s}}{T_{1N}s+1}\\ \frac{K_{21}e^{-\tau_{21}s}}{T_{21}s+1} & \frac{K_{22}e^{-\tau_{22}s}}{T_{22}s+1} & \cdots & \frac{K_{2N}e^{-\tau_{2N}s}}{T_{2N}s+1}\\ \vdots & \vdots & \ddots & \vdots\\ \frac{K_{N1}e^{-\tau_{n1}s}}{T_{N1}s+1} & \frac{K_{N2}e^{-\tau_{n2}s}}{T_{N2}s+1} & \cdots & \frac{K_{NN}e^{-\tau_{NN}s}}{T_{NN}s+1}\end{bmatrix} \tag{1}$$

where,

K_{ij}, T_{ij} and τ_{ij} $(i,j=1,2,\cdots,N)$ represent the steady-state gain, the time constant and the lag time of the corresponding subsystem, respectively.

By discretizing the model in Eq.(1), the difference equation of the large-scale coupled system is obtained

$$Y_{PM}(k)=Y_{P0}(k)-A_{P0}u_{P0}(k-1)+H\mu(k) \tag{2}$$

where,

$$Y_{PM}(k)=\left[y_{1,PM}(k),y_{2,PM}(k),\cdots,y_{i,PM}(k),\cdots y_{N,PM}(k)\right]^T$$
$$Y_{P0}(k)=\left[y_{1,P0}(k),y_{2,P0}(k),\cdots,y_{i,P0}(k),\cdots y_{N,P0}(k)\right]^T$$
$$\mu(k)=[\mu_1(k),\mu_2(k),\cdots,\mu_N(k)]^T,\quad H=A_{PM}F$$
$$A_{P0}=\begin{bmatrix}A_{11,P0} & A_{12,P0} & \cdots & A_{1N,P0}\\ A_{21,P0} & A_{22,P0} & \cdots & A_{2N,P0}\\ \vdots & \vdots & \ddots & \vdots\\ A_{N1,P0} & A_{N2,P0} & \cdots & A_{NN,P0}\end{bmatrix},$$

$$\mathrm{H} = \begin{bmatrix} H_{11} & H_{12} & \cdots & H_{1N} \\ H_{21} & H_{22} & \cdots & H_{2N} \\ \vdots & \vdots & \ddots & \vdots \\ H_{N1} & H_{N2} & \cdots & H_{NN} \end{bmatrix}$$

$$A_{PM} = \begin{bmatrix} A_{11,PM} & A_{12,PM} & \cdots & A_{1N,PM} \\ A_{21,PM} & A_{22,PM} & \cdots & A_{2N,PM} \\ \vdots & \vdots & \ddots & \vdots \\ A_{N1,PM} & A_{N2,PM} & \cdots & A_{NN,PM} \end{bmatrix},$$

$$\mathrm{F} = \begin{bmatrix} F_{1,G} & & & \\ & F_{2,G} & & \\ & & \ddots & \\ & & & F_{N,G} \end{bmatrix}$$

$$A_{ij,PM} = \begin{bmatrix} a_{ij,1} \\ a_{ij,2} - a_{ij,1} a_{ij,1} \\ \vdots \vdots \ddots \\ a_{ij,M} - a_{ij,M-1} a_{ij,M-1} - a_{ij,M-2} \cdots a_{ij,1} \\ \vdots \vdots \ddots \vdots \\ a_{ij,P} - a_{ij,P-1} a_{ij,P-1} - a_{ij,P-2} \cdots a_{ij,P-M+1} \end{bmatrix}$$

$$A_{ij,P0} = \left[a_{ij,1}, a_{ij,2}, \cdots, a_{ij,M}, \cdots, a_{ij,P}\right]^T, \quad k = 1, 2, \cdots P, \quad i, j = 1, 2, \cdots N.$$

where,

$y_{i,PM}(k)$ is the output prediction of the i subsystem at time instant k, and $y_{i,P0}(k)$ is the initial output prediction of the i subsystem at time instant k. $u_{i,P0}(k-1)$ represents the input of the i subsystem at time instant $k-1$. $\mu_i(k)$ represents the coefficient matrix of the basis function of the i subsystem at time instant k. P, M are the prediction horizon and control horizon of the DPFC. N is the model length of the DPFC. $a_{ij,1}, \cdots, a_{ij,P}$ denote the step response value of the corresponding subsystem, and $F_{i,G}$ is a matrix that consists of the basic functions of each subsystem.

Based on the strategy of distributed control, the large-scale system described in Eq.(2) can be further decomposed into N coupled subsystems, where the control model and performance index of the i subsystem can be described as follows:

$$y_{i,PM}(k) = y_{i,P0}(k) - A_{ij,P0} u_{i,P0}(k-1) + H_{ii}(k)\mu_i(k) + \sum_{j=1, j\neq i}^{N} H_{ij}(k)\mu_j(k) \tag{3}$$

$$\min J_i(k) = \left\| ref_i(k) - y_{i,PM}(k) \right\|_{Q_i}^2 \tag{4}$$

where,

$$y_{i,PM}(k) = \left[y_{i,PM}(k+1/k), \cdots, y_{i,PM}(k+P/k)\right]^T,$$
$$y_{i,P0}(k) = \left[y_{i,P0}(k+1/k), \cdots, y_{i,P0}(k+P/k)\right]^T,$$
$$\mu_i(k) = [\mu_{i,1}(k), \mu_{i,2}(k), \ldots, \mu_{i,G}^l(k)]^T,$$
$$\mu_j(k) = [\mu_{j,1}(k), \mu_{j,2}(k), \ldots, \mu_{j,G}(k)]^T,$$
$$ref_i(k) = [ref_i(k+1), ref_i(k+2), \cdots, ref_i(k+P)]^T.$$

$\sum_{j=1, j\neq i}^{N} H_{ij}(K)\mu_j(k)$ is the coupling effect of the input of the j subsystem on the output of the i subsystem at time instant k. $H_{ii}(k)$ represents the calculation matrix of the i subsystem at time instant k, and $H_{ij}(k)$ denotes the calculation matrix of the coupling effect of the j subsystem on the i subsystem at time instant k. $ref_i(k+1), ref_i(k+2), \cdots ref_i(k+P)$ are the reference trajectory of the i subsystem. Q_i is the corresponding error weighting matrix of the i subsystem.

Based on the Nash optimization strategy, the performance index $J_i(k)$ of the i subsystem can be optimized. And the Nash optimal solution of the i subsystem is obtained as

$$\mu_i^*(k) = D_{ii}[ref_i(k) - y_{i,P0}(k) + A_{i,P0} u_{i,P0}(k-1) - \sum_{j=1, j\neq i}^{n} H_{ij}(k)\mu_j^*(k)] \tag{5}$$

where,

$$D_{ii} = (H_{ii}^T Q_i H_{ii})^{-1} H_{ii}^T Q_i$$

Further, the Nash optimal solution for the i subsystem at time instant k for a new iteration is

$$\mu_i^{l+1}(k) = D_{ii}[ref_i(k) - y_{i,P0}(k) + A_{i,P0} u_{i,P0}(k-1) - \sum_{j=1, j\neq i}^{n} H_{ij}(k)\mu_j^l(k)] \tag{6}$$

If the algorithm satisfies the convergence condition of the Nash optimization strategy, the Nash optimal solution of the whole DPFC system at time instant k can be expressed as

$$\mu^{l+1}(k) = D_1[ref(k) - Y_{P0}(k) + A_{P0} u_{P0}(k-1)] + D_2 \mu^l(k) \tag{7}$$

where,

$$D_1 = \begin{bmatrix} D_{11} & & & \\ & D_{22} & & \\ & & \ddots & \\ & & & D_{NN} \end{bmatrix},$$

$$D_2 = \begin{bmatrix} 0 & D_{11}H_{12} & \cdots & D_{11}H_{1N} \\ D_{22}H_{21} & 0 & \cdots & D_{22}H_{2N} \\ \vdots & \vdots & \ddots & \vdots \\ D_{NN}H_{N1} & D_{NN}H_{N2} & \cdots & 0 \end{bmatrix}$$

Here, the basis function is selected as step function. Meanwhile, the number of basic functions is chosen as 1, then the control input of the i subsystem at time instant k is

$$u^{l+1}(k) = \mu^{l+1}(k) = D_1[ref(k) - Y_{P0}(k) + A_{P0} u_{P0}(k-1)] + D_2 \mu^l(k) \tag{8}$$

B. CONVERGENCE THEOREM OF ALGORITHM ITERITION

By analyzing the convergence of the above DPFC algorithm iteration, the following convergence theorem is obtained.

Theorem: For the DPFC system in which the Nash optimal strategy is employed, the absolute value of the spectral radius of D_2 must be less than 1, i.e., $|\rho(D_2) < 1|$.

Proof: It can be known that $ref(k)$, $y_{PO}(k)$ are known or measurable at time instant k, such that $D_1[ref(k) - Y_{P0}(k) + A_{P0}u_{P0}(k-1)]$ is also a constant at time instant k. Therefore, the convergence of the DPFC algorithm mainly depends on the second term in Eq.(8), that is, $D_2\mu^l(k)$. According to the above analysis, the convergence condition need to be satisfied in algorithm iteration is derived as $|\rho(D_2) < 1|$.

III. BFPID-DPFC ALGORITHM

In this section, the derivation of the improved BFPID-DPFC strategy will be introduced in detail.

A. ESTABLISHMENT OF PREDICTION MODEL

Refer to the derivation in the conventional DPFC, the prediction model of the i subsystem is obtained.

$$y_{i,PM}(k) = y_{i,P0}(k) - A_{ij,P0}u_{i,P0}(k-1) + H_{ii}(k)\,\mu_i(k) + \sum_{j=1,j\neq i}^{N} H_{ij}(k)\mu_j(k) \tag{9}$$

By employing the PID operator, the weighting coefficient of the basis function and the control weighting factor λ into the performance index, the new objective function of the i subsystem can be expressed as follows.

$$\min \tilde{J}_i(k) = E_0^i(k)^T K_I^i E_0^i(k) + \Delta E_0^i(k)^T K_p^i \Delta E_0^i(k) + \Delta^2 E_0^i(k)^T K_d^i \Delta^2 E_0^i(k) + \lambda \mu_{i,M}^T \mu_{i,M} \tag{10}$$

where,

$$\begin{aligned} E_0^i(k) &= \left[ref_i(k+1) - y_{i,PM}(k+1/k)\right] \\ &= \left[ref_i(k+1) - W_i(k) - H_{ii}(k)\,\mu_i(k)\right] \\ \Delta E_0^i(k) &= \left[\Delta ref_i(k+1) - \Delta y_{i,PM}(k+1/k)\right] \\ \Delta^2 E_0^i(k) &= \left[\Delta^2 ref_i(k+1) - \Delta^2 y_{i,PM}(k+1/k)\right] \\ W_i(k) &= y_{i,P0}(k) - A_{ij,P0}u_{i,P0}(k-1) + \sum_{j=1,j\neq i}^{N} H_{ij}(k)\mu_j(k) \\ \mu_{i,M} &= [\mu_i(k), \mu_i(k+1), \cdots, \mu_i(k+M-1)]^T \end{aligned}$$

$K_p^i = diag(k_p^i, \cdots, k_p^i)$, $K_I^i = diag(k_I^i, \cdots, k_I^i)$, $K_d^i = diag(k_d^i, \cdots, k_d^i)$ $E_0^i(k)$ is the difference value between the reference trajectory and the output prediction of the i subsystem, and Δ denotes the difference operator.

The corresponding shift matrix is introduced as

$$S = \begin{bmatrix} H_{ii}(k) & 0 & 0 \ \cdots & 0 \\ H_{ii}(k+1) & H_{ii}(k) & 0 \ \cdots & 0 \\ \vdots & \vdots & \ddots \ \vdots & 0 \\ H_{ii}(k+M) & \cdots & \cdots\cdots & H_{ii}(k) \\ H_{ii}(k+M+1) & \cdots & \cdots\cdots & H_{ii}(k)+H_{ii}(k+1) \\ \vdots & \ddots & \ddots \ \vdots & \vdots \\ H_{ii}(k+P-1) & H_{ii}(k+P-2) & \cdots\cdots & \sum_{\delta=0}^{P-1} H_{ii}(k+\delta) \end{bmatrix}_{P\times M},$$

$$S_1 = \begin{bmatrix} 1 & 0 & \cdots & 0 & 0 \\ -1 & 1 & 0 & \cdots & 0 \\ 0 & -1 & 1 & \ddots & \vdots \\ \vdots & \ddots & \ddots & \ddots & 0 \\ 0 & \cdots & 0 & -1 & 1 \end{bmatrix}_{P\times P}.$$

Further, the following formula is acquired.

$$\begin{cases} \Delta E_0^i(k) = S_1 E_0^i(k) \\ \Delta^2 E_0^i(k) = S_1 \Delta E_0^i(k) = S_1^2 E_0^i(k) \end{cases} \tag{11}$$

Then the performance index of the i system can be rewritten as

$$\min \tilde{J}_i(k) = \left(ref_i(k) - W_i(k) - S\mu_{i,M}\right)^T \times Q_{i,1}\left(ref_i(k) - W_i(k) - S\mu_{i,M}\right) + \lambda \mu_{i,M}^T \mu_{i,M} \tag{12}$$

where,

$$Q_{i,1} = K_I^i + K_p^i S_1^T S_1 + K_d^i (S_1^2)^T (S_1^2)$$

B. DESIGN OF BFPID-DPFC

By letting the derivative of the performance index $\tilde{J}_i(k)$ as 0, i.e., $\frac{\partial \tilde{J}_i(k)}{\partial \mu_{i,M}(k)} = 0$, the Nash optimal solution of the i subsystem is derived.

$$\begin{aligned} \mu_{i,M}^* &= D_{ii,1}\left(ref_i(k) - W_i(k)\right) \\ &= D_{ii,1}[ref_i(k) - y_{i,P0}(k) + A_{i,P0}u_{i,P0}(k-1) \\ &\quad - \sum_{j=1,j\neq i}^{n} H_{ij}(k)\,\mu_j^*(k)] \end{aligned} \tag{13}$$

where,

$$D_{ii,1} = (\lambda + S^T Q_{i,1} S)^{-1} S^T Q_{i,1}$$

The Nash optimal control increment of the i subsystem at time instant k is obtained.

$$\mu_i^*(k) = [1, 0, \cdots, 0]\mu_{i,M}^*(k) \tag{14}$$

Further, the Nash optimal solution for the i subsystem at time instant k for a new iteration is expressed as

$$\mu_{i,M}^{l+1}(k) = [1, 0, \cdots, 0]\,D_{ii,1}[ref_i(k) - y_{i,P0}(k) + A_{i,P0}u_{i,P0}(k-1) - \sum_{j=1,j\neq i}^{n} H_{ij}(k)\,\mu_j^l(k)] \tag{15}$$

Finally, the Nash optimal solution of the entire DPFC system at time instant k can be obtained if the convergence condition of the Nash optimization strategy is satisfied in the presented algorithm.

$$\mu_M^{l+1}(k) = D_3[ref(k) - Y_{P0}(k) + A_{P0}u_{P0}(k-1)] + D_4\mu_j^l(k) \tag{16}$$

where,

$$D_3 = \begin{bmatrix} D_{11,1} & & 0 \\ & D_{22,1} & \\ & & \ddots & \\ 0 & & & D_{NN,1} \end{bmatrix},$$

$$D_4 = \begin{bmatrix} 0 & D_{11,1}H_{12} & \cdots & D_{11,1}H_{1N} \\ D_{22,1}H_{21} & 0 & \cdots & D_{22,1}H_{2N} \\ \vdots & \vdots & \ddots & \vdots \\ D_{NN,1}H_{N1} & D_{NN,1}H_{N2} & \cdots & 0 \end{bmatrix}$$

$$\mu_M^{l+1}(k) = \left[\mu_{1,M}^{l+1}(k), \mu_{2,M}^{l+1}(k), \cdots, \mu_{N,M}^{l+1}(k)\right]^T$$

By choosing the basis function as step function and the number of the basic functions as 1, the control input of the i subsystem at time instant k is

$$u^{l+1}(k) = \mu^{l+1}(k) = D_3[ref(k) - Y_{P0}(k) + A_{P0}u_{P0}(k-1)] + D_4\mu_j^l(k) \quad (17)$$

IV. SIMULATION STUDY

In order to evaluate the effectiveness of the proposed DPFC strategy, the conventional DPFC method is employed as the comparison in this section.

Consider a large-scale coupled system with three inputs and three outputs [30]

$$G(s) = \begin{bmatrix} \frac{e^{-4s}}{79s+1} & \frac{e^{-6s}}{87s+1} & \frac{e^{-4s}}{120s+1} \\ \frac{-1.25e^{-2s}}{33s+1} & \frac{3.75e^{-6s}}{36s+1} & \frac{e^{-3s}}{38s+1} \\ \frac{-2e^{-2s}}{120s+1} & \frac{2e^{-4s}}{145s+1} & \frac{3.5e^{-2s}}{85s+1} \end{bmatrix} \quad (18)$$

As to the selected coupling system, we need to decompose it into subsystems according to the actual industrial situations, and the obtained three subsystems are

$$\text{Subsystem1}: \quad G_1(s) = \frac{e^{-4s}}{79s+1} \quad (19)$$

$$\text{Subsystem2}: \quad G_2(s) = \frac{3.75e^{-6s}}{36s+1} \quad (20)$$

$$\text{Subsystem3}: \quad G_3(s) = \frac{3.5e^{-2s}}{85s+1} \quad (21)$$

The set-point is chosen as 5 for both approaches. Meanwhile, the output disturbance with amplitude of -1 is added to the whole system at time instant $k = 500$ to test the corresponding control performance. The error precision is specified as 0.01 for the employed Nash optimization strategy, and Tab.1 lists the control parameters for two DPFC methods.

To verify the validity of the BFPID-DPFC algorithm further, here we introduce two cases, that is, the case under model/plant match and cases under model/plant mismatch.

(1) model/plant match

TABLE 1. Control parameters of two DPFC approaches.

Parameters	BFPID-DPFC	Traditional DPFC
P	8	
M	3	
E	1	
N	1000	
Ts	20s	
α	1	
β	0.95	
λ	0.2	\
$k_p^1\ k_i^1\ k_d^1$	0.47，0.18，8.6	\
$k_p^2\ k_i^2\ k_d^2$	0.52，0.11，12.4	\
$k_p^3\ k_i^3\ k_d^3$	0.53，0.08，11.5	\

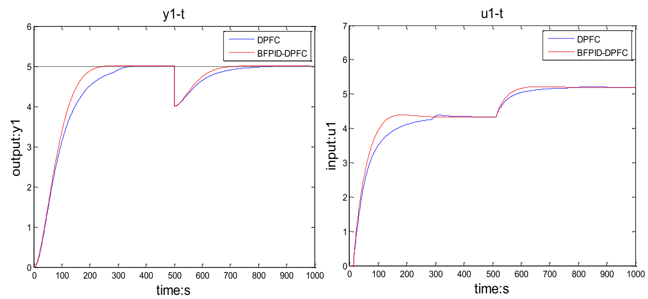

FIGURE 1. Output and input responses of the subsystem 1.

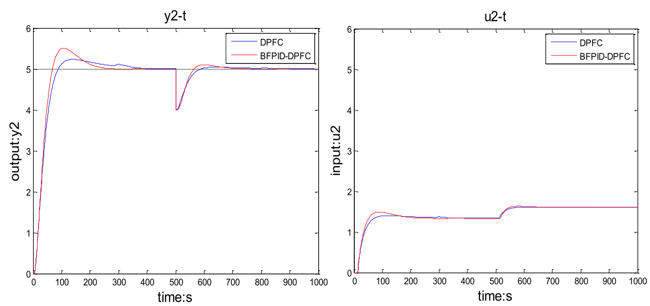

FIGURE 2. Output and input responses of the subsystem 2.

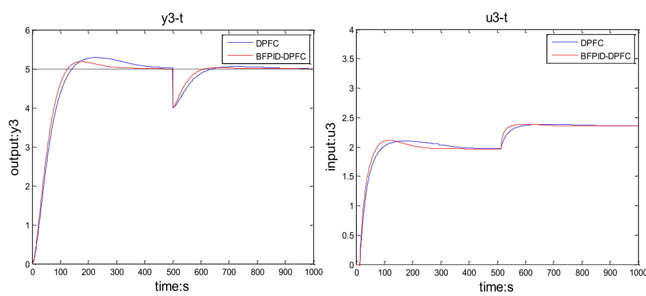

FIGURE 3. Output and input responses of the subsystem 3.

Figs.1∼3 show the corresponding output and input responses for subsystems.

Here, the corresponding statistical performance indexes for subsystems are shown in Tab.2

TABLE 2. Performance indexes for two strategies.

Time index	BFPID-DPFC	Traditional DPFC
Rise time: t_r	Subsystem1:279s	Subsystem1:319s
	Subsystem2:79s	Subsystem2:91s
	Subsystem3:97s	Subsystem3:104s
Peak time: t_p	Subsystem1:70s	Subsystem1:83s
	Subsystem2:39s	Subsystem2:44s
	Subsystem3:49s	Subsystem3:52s
Settling time: t_s	Subsystem1:410s	Subsystem1:363s
	Subsystem2:99s	Subsystem2:102s
	Subsystem3:131s	Subsystem3:156s
Peak value: h_p	Subsystem1:5.018	Subsystem1:5.029
	Subsystem2:5.558	Subsystem2:5.283
	Subsystem3:5.161	Subsystem3:5.272
Overshoot: σ	Subsystem1:0.36%	Subsystem1:0.58%
	Subsystem2:11.16%	Subsystem2:5.66%
	Subsystem3:3.22%	Subsystem3:5.44%
Recovery time: t_h	Subsystem1:625s	Subsystem1:688s
	Subsystem2:573s	Subsystem2:628s
	Subsystem3:586s	Subsystem3:635s

From Tab.2 and Figs.1∼3, we can obtain the following conclusion.

1) As to the settling time, the rise time, the delay time and the peak time, the BFPID-DPFC algorithm provides better performance than the conventional DPFC on the whole, which indicates that the speed ability of the BFPID-DPFC scheme is improved.
2) In terms of the overshoot, two approaches offer the similar performance, which implies that the dynamic stability of the two DPFC methods is similar.
3) For the recovery time after encountering the disturbance, the proposed DPFC method behaves better than the traditional DPFC, which means that the robustness of the presented algorithm is modified.

To sum up, the ensemble control performance of the BFPID-DPFC approach is superior to the conventional method under model/plant matched case.

(2) model/plant mismatch

It is known that disturbances and various uncertainties are inevitable in practice, which may cause model/plant mismatch. Here, three model/plant mismatched groups are generated by Monte Carlo method to evaluate the control performance for both strategies (the maximum degree of mismatch is ±30%).

1)The first group

$$\text{Subsystem1}: \quad G_1(s) = \frac{1.135e^{-3.278s}}{82s+1} \tag{22}$$

$$Subsystem2: \quad G_2(s) = \frac{3.235e^{-6.235s}}{31.25s+1} \tag{23}$$

$$Subsystem3: \quad G_3(s) = \frac{3.526e^{-2.163s}}{92.36s+1} \tag{24}$$

The relevant responses of two approaches under the first group are shown in Figs.4∼6.

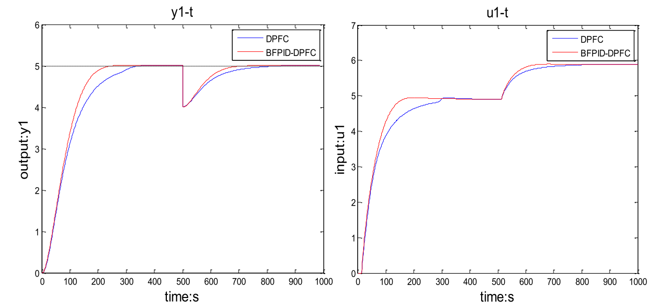

FIGURE 4. Output and input responses of the subsystem 1 under the first group.

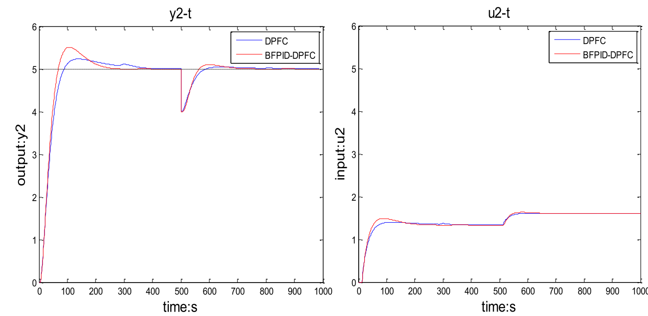

FIGURE 5. Output and input responses of the subsystem 2 under the first group.

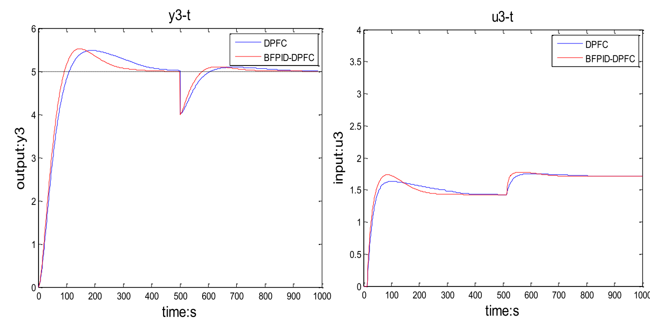

FIGURE 6. Output and input responses of the subsystem 3 under the first group.

2)The second group

$$Subsystem1: \quad G_1(s) = \frac{0.982e^{-3.46s}}{78.231s+1} \tag{25}$$

$$Subsystem2: \quad G_2(s) = \frac{3.756e^{-6.98s}}{38.36s+1} \tag{26}$$

$$Subsystem3: \quad G_3(s) = \frac{3.812e^{-2.21s}}{85.96s+1} \tag{27}$$

Figs.7∼9 display the corresponding responses of subsystems for two schemes under the second group.

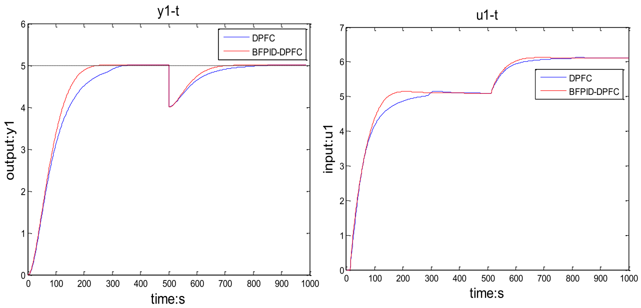

FIGURE 7. Output and input responses of the subsystem 1 under the second group.

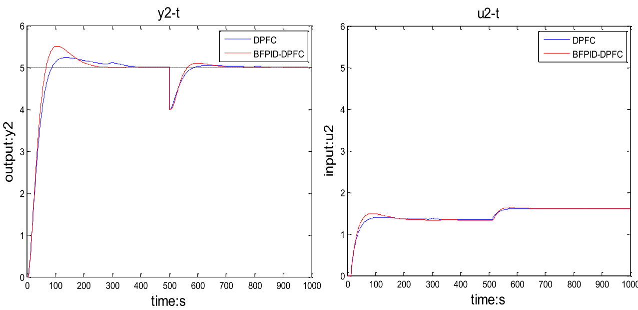

FIGURE 8. Output and input responses of the subsystem 2 under the second group.

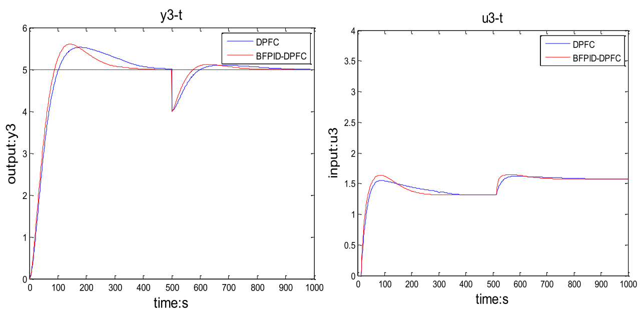

FIGURE 9. Output and input responses of the subsystem 3 under the second group.

3)The third group

$$Subsystem1: \quad G_1(s) = \frac{1.154e^{-3.741s}}{84.472s+1} \tag{28}$$

$$Subsystem2: \quad G_2(s) = \frac{3.012e^{-4.315s}}{39.358s+1} \tag{29}$$

$$Subsystem3: \quad G_3(s) = \frac{2.547e^{-2.388s}}{74.623s+1} \tag{30}$$

The relevant output and input responses of subsystems for both methods under the model/plant match are as below.

Here, the corresponding statistical performance indexes for subsystems in the case of mismatch of three models are shown in Tab.3. where, a represents subsystem 1, b represents subsystem 2, and c represents subsystem 3.

From Figs. 4∼12 and Tab.3, it can be easily seen that the BFPID-DPFC strategy behaves better than the traditional

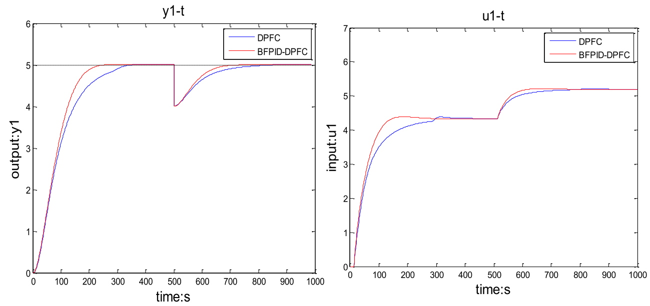

FIGURE 10. Output and input responses of the subsystem 1 under the third group.

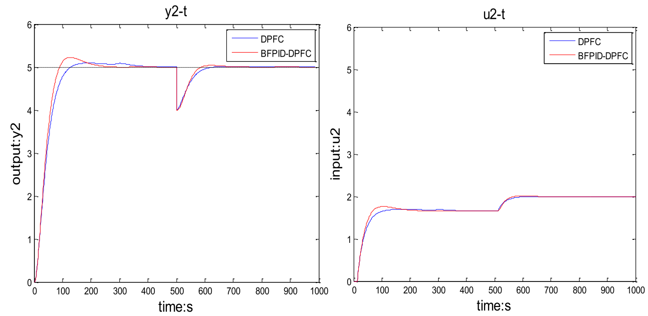

FIGURE 11. Output and input responses of the subsystem 2 under the third group.

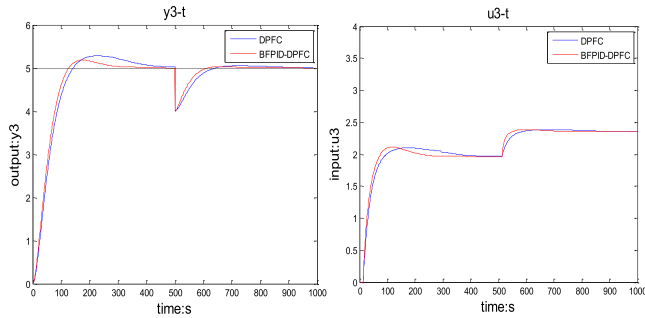

FIGURE 12. Output and input responses of the subsystem 3 under the third group.

DPFC method in the aspects of the settling time, the overshoot and the recovery time as a whole, which verifies the superiority of the proposed DPFC scheme under model/plant mismatched cases. The details are as follows

1.Under the model/plant mismatch, for the settling time, the rise time, the delay time and the peak time, the BFPID-DPFC algorithm provides better performance than the conventional DPFC on the whole, which indicates that the speed ability of the BFPID-DPFC scheme is improved.

2.Under the model/plant mismatch, and as to overshoot, two approaches offer the similar performance, which implies that the dynamic stability of two DPFC methods is parallel.

3.Under the model/plant mismatch, in terms of the the recovery time after encountering the disturbance, the proposed DPFC method behaves better than the traditional DPFC, which means that the robustness of the presented algorithm is modified.

TABLE 3. Performance indexes for two strategies under the model/plant mismatch.

Time index	model/plant mismatch 1		model/plant mismatch 2		model/plant mismatch 3	
	BFPID-DPFC	DPFC	BFPID-DPFC	DPFC	BFPID-DPFC	DPFC
Rise time: t_r	a:282s	a:326s	a:280s	a:320s	a:285s	a:331s
	b:82s	b:134s	b:85s	b:104s	b:83s	b:116s
	c:126s	c:135s	c:106s	c:118s	c:120s	c:141s
Peak time: t_p	a:419s	a:389s	a:378s	a:395s	a:398s	a:402s
	b:107s	b:189s	b:97s	b:159s	b:105s	b:143s
	c:139s	c:195s	c:149s	c:185s	c:149s	c:235s
Settling time: t_s	a:169s	a:236s	a:164s	a:232s	a:172s	a:240s
	b:69s	b:82s	b:129s	b:91s	b:183s	b:117s
	c:89s	c:256s	c:219s	c:266s	c:95s	c:162s
Peak value: h_p	a:5.018	a:5.029	a:5.014	a:5.018	a:5.014	a:5.017
	b:5.247	b:5.138	b:5.251	b:5.127	b:5.561	b:5.247
	c:5.250	c:5.297	c:5.256	c:5.262	c:5.138	c:5.256
Overshoot: σ	a:0.36%	a:0.58%	a:0.28%	a:0.36%	a:0.28%	a:0.34%
	b:4.94%	b:2.76%	b:5.02%	b:2.54%	b:11.22%	b:4.94%
	c:4.95%	c:5.94%	c:5.12%	c:5.24%	c:2.76%	c:5.12%
Recovery time: t_h	a:638s	a:682s	a:625s	a:678s	a:632s	a:679s
	b:578s	b:618s	b:572s	b:626s	b:586s	b:619s
	c:592s	c:622s	c:586s	c:615s	c:582s	c:624s

In a word, the BFPID-DPFC strategy not only solves the disturbances in practice but also provides improved ensemble control performance.

V. CONCLUSION

In this paper, an improved DPFC with basic function and PID control structure is proposed for the large-scale coupled system. By combining the PID factor with the feedback error, introducing the control weighting factor and the weighting coefficient of the basic function, a novel performance index is developed for the presented algorithm firstly. Then the coupling effect between subsystems is eliminated by distributed optimization according to the Nash game theory, and the enhanced DPFC strategy is obtained finally. The simulations on a large-scale coupled system prove the validity of the BFPID-DPFC approach, and the results show that BFPID-DPFC algorithm not only solves the disturbances in practice but also provides improved ensemble control performance.

This BFPID-DPFC method has a significant improvement on the rapidity and anti-interference ability of the system, which can be used for some occasions with high rapidity requirements, such as electromechanical coupling system. Furthermore, the overshoot of large-scale system can be further improved, which makes the method more widely used.

ACKNOWLEDGMENT

This work was supported by the National Natural Science Foundation of China under Grant 61773146.

REFERENCES

[1] R. Zhang and S. Wang, "Support vector machine based predictive functional control design for output temperature of coking furnace," *J. Process Control*, vol. 18, no. 5, pp. 439–448, Jun. 2008.

[2] C. E. García, D. M. Prett, and M. Morari, "Model predictive control: Theory and practice—A survey," *Automatica*, vol. 25, no. 3, pp. 335–348, May 1989.

[3] P. Trodden and A. Richards, "Cooperative distributed MPC of linear systems with coupled constraints," *Automatica*, vol. 49, no. 2, pp. 479–487, Feb. 2013.

[4] P.-D. Moroşan, R. Bourdais, D. Dumur, and J. Buisson, "A distributed MPC strategy based on Benders' decomposition applied to multi-source multi-zone temperature regulation," *J. Process Control*, vol. 21, no. 5, pp. 729–737, Jun. 2011.

[5] S. Li, Y. Zhang, and Q. Zhu, "Nash-optimization enhanced distributed model predictive control applied to the Shell benchmark problem," *Inf. Sci.*, vol. 170, nos. 2–4, pp. 329–349, Feb. 2005.

[6] Y. Song, C. Liu, and W. Wang, "Domain selective precoding in 3-D massive MIMO systems," *IEEE J. Sel. Topics Signal Process.*, vol. 13, no. 5, pp. 1103–1118, Sep. 2019.

[7] E. Kayacan, E. Kayacan, H. Ramon, and W. Saeys, "Distributed nonlinear model predictive control of an autonomous tractor–trailer system," *Mechatronics*, vol. 24, no. 8, pp. 926–933, Dec. 2014.

[8] B. T. Stewart, S. J. Wright, and J. B. Rawlings, "Cooperative distributed model predictive control for nonlinear systems," *J. Process Control*, vol. 21, no. 5, pp. 698–704, Jun. 2011.

[9] H. Li, Y. Shi, and W. Yan, "On neighbor information utilization in distributed receding horizon control for consensus-seeking," *IEEE Trans. Cybern.*, vol. 46, no. 9, pp. 2019–2027, Sep. 2016.

[10] W. Ao, Y. Song, and C. Wen, "Adaptive robust fault tolerant control design for a class of nonlinear uncertain MIMO systems with quantization," *ISA Trans.*, vol. 68, pp. 63–72, May 2017.

[11] Y. Gao, L. Dai, and Y. Xia, "Cooperative distributed model predictive control of multiple coupled linear systems," *IET Control Theory Appl.*, vol. 9, no. 17, pp. 2561–2567, Nov. 2015.

[12] E. Camponogara, D. Jia, B. H. Krogh, and S. Talukdar, "Distributed model predictive control," *IEEE Control Syst.*, vol. 22, no. 1, pp. 44–52, Feb. 2002.

[13] P. D. Christofifides, J. Liu, and D. L. Pena, *Networked and Distributed Predictive Control: Methods and Nonlinear Process Network Applications*. London, U.K.: Springer, 2011.

[14] A. Venkat, I. Hiskens, J. Rawlings, and S. Wright, "Distributed MPC strategies with application to power system automatic generation control," *IEEE Trans. Control Syst. Technol.*, vol. 16, no. 6, pp. 1192–1206, Nov. 2008.

[15] M. Mercangöz and F. J. Doyle, "Distributed model predictive control of an experimental four-tank system," *J. Process Control*, vol. 17, no. 3, pp. 297–308, Mar. 2007.
[16] K. J. Åström and T. Hägglund, "The future of PID control," *Control Eng. Pract.*, vol. 9, no. 11, pp. 1163–1175, Nov. 2001.
[17] C. Knospe, "PID control," *IEEE Control Syst. Mag.*, vol. 26, no. 1, pp. 30–31, Feb. 2006.
[18] Y. Li, K. H. Ang, and G. C. Y. Chong, "PID control system analysis and design," *IEEE Control Syst.*, vol. 26, no. 1, pp. 32–41, Feb. 2006.
[19] C. C. Hang, K. J. Astrom, and W. K. Ho, "Refinements of the Ziegler–Nichols tuning formula," *IEE Proc. D, Control Theory Appl.*, vol. 38, no. 2, pp. 111–118, Mar. 1991.
[20] W. Ho, O. Gan, E. Tay, and E. Ang, "Performance and gain and phase margins of well-known PID tuning formulas," *IEEE Trans. Control Syst. Technol.*, vol. 4, no. 4, pp. 473–477, Jul. 1996.
[21] D. L. Laughlin, D. E. Rivera, and M. Morari, "Smith predictor design for robust performance," *Int. J. Control*, vol. 46, no. 2, pp. 477–504, Aug. 1987.
[22] P. S. Fruehauf, I.-L. Chien, and M. D. Lauritsen, "Simplified IMC-PID tuning rules," *ISA Trans.*, vol. 33, no. 1, pp. 43–59, May 1994.
[23] K. J. Åström and T. Hägglund, *Automatic Tuning of PID Controllers*. Research Triangle, NC, USA: Instrument Society of America, 1988.
[24] K. Eltag, M. S. Aslamx, and R. Ullah, "Dynamic stability enhancement using fuzzy PID control technology for power system," *Int. J. Control, Automat. Syst.*, vol. 17, no. 1, pp. 234–242, Jan. 2019.
[25] T. Abut and S. Soyguder, "Real-time control and application with self-tuning PID-type fuzzy adaptive controller of an inverted pendulum," *Ind. Robot*, vol. 46, no. 1, pp. 159–170, Jan. 2019.
[26] R. Zhang, A. Xue, S. Wang, and Z. Ren, "An improved model predictive control approach based on extended non-minimal state space formulation," *J. Process Control*, vol. 21, no. 8, pp. 1183–1192, Sep. 2011.
[27] A. Andrášik, A. Mészáros, and S. De Azevedo, "On-line tuning of a neural PID controller based on plant hybrid modeling," *Comput. Chem. Eng.*, vol. 28, no. 8, pp. 1499–1509, Jul. 2004.
[28] K. Kwok, M. C. Ping, and P. Li, "A model-based augmented PID algorithm," *J. Process Control*, vol. 10, no. 1, pp. 9–18, Feb. 2000.
[29] R. Zhang and Q. Jin, "Design and implementation of hybrid modeling and PFC for oxygen content regulation in a coke furnace," *IEEE Trans. Ind. Informat.*, vol. 14, no. 6, pp. 2335–2342, Jun. 2018.
[30] G. Liu, S. Abdul, and A. A. Goldenberg, "Distributed control of modular and reconfigurable robot with torque sensing," *Robotica*, vol. 26, no. 1, pp. 75–84, Jan. 2008.
[31] B. Srinivasarao, G. Sreenivasan, and S. Sharma, "Compensation of voltage distribunces in SMIB system using ANN based DPFC controller," in *Proc. Int. Conf. Signal Process., Commun., Power Embedded Syst. (SCOPES)*, Oct. 2016, pp. 563–567.
[32] K. Worthmann, C. M. Kellett, P. Braun, L. Grune, and S. R. Weller, "Distributed and decentralized control of residential energy systems incorporating battery storage," *IEEE Trans. Smart Grid*, vol. 6, no. 4, pp. 1914–1923, Jul. 2015.
[33] D. Wang and R. Zhang, "Design of distributed PID-type dynamic matrix controller for fractional-order systems," *Int. J. Syst. Sci.*, vol. 49, no. 2, pp. 435–448, Jan. 2018.
[34] Y. Zheng, S. E. Li, K. Li, F. Borrelli, and J. K. Hedrick, "Distributed model predictive control for heterogeneous vehicle platoons under unidirectional topologies," *IEEE Trans. Control Syst. Technol.*, vol. 25, no. 3, pp. 899–910, May 2017.
[35] Y. S. Zhang, Z. Z. Zhong, and S. K. Zhong, "Distributed optimization algorithm for predictive functional control," *Process Automat. Instrum.*, vol. 35, no. 07, pp. 72–77, Jul. 2014.
[36] J. Zhan, Z.-P. Jiang, Y. Wang, and X. Li, "Distributed model predictive consensus with self-triggered mechanism in general linear multiagent systems," *IEEE Trans. Ind. Informat.*, vol. 15, no. 7, pp. 3987–3997, Jul. 2019.
[37] R. Zhang, S. Wu, Z. Cao, J. Lu, and F. Gao, "A systematic min-max optimization design of constrained model predictive tracking control for industrial processes against uncertainty," *IEEE Trans. Control Syst. Technol.*, vol. 26, no. 6, pp. 2157–2164, Nov. 2018.
[38] A. H. Kaveh and D. Robert, "Decentralized controllers for robust stabilization of periodic orbits of hybrid systems: Application to bipedal walking," *IEEE Trans. Control Syst. Techn.*, vol. 25, no. 4, pp. 1153–1167, Aug. 2017.
[39] R. Zhang and F. Gao, "Multivariable decoupling predictive functional control with non-zero–pole cancellation and state weighting: Application on chamber pressure in a coke furnace," *Chem. Eng. Sci.*, vol. 94, pp. 30–43, May 2013.
[40] P. Ortner and L. D. Re, "Predictive control of a diesel engine air path," *IEEE Trans. Control Syst. Technol.*, vol. 15, no. 3, pp. 449–456, May 2007.

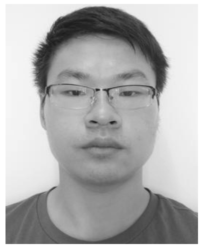

ZHE YU is currently pursuing the master's degree with the School of Automation, Hangzhou Dianzi University. His current research interests include predictive control and distributed control.

JIANJUN BAI received the Ph.D. degree in control science and engineering from Zhejiang University, Hangzhou, China, in 2012. He is currently an Associate Professor with the Institute of Information and Control, Hangzhou Dianzi University, Hangzhou. His research interests include robust control, robot control, and fuzzy neural systems.

HONGBO ZOU is currently an Associate Professor with the Automation Department, Hangzhou Dianzi University, Hangzhou. He has published more than 30 articles on robust control and model predictive control. His research interests include robust control, model predictive control, and control system design.